

**Review: Low transformation temperature weld filler for tensile residual stresses reduction**

S. W. Ooi\*, J.E. Garnham and T. I. Ramjaun

Department of Materials Science and Metallurgy, University of Cambridge, 27 Charles Babbage Road, Cambridge CB3 0FS, United Kingdom

Corresponding author contact details

Email: [swo23@cam.ac.uk](mailto:swo23@cam.ac.uk)

Tel: 01223334336

Fax: 01223334567

---

**Abstract**

An attractive, alternative approach for the reduction of harmful residual stresses in weld zones is reviewed, which utilises low temperature, solid-state, displacive phase transformations in steel. The theory, latest concepts and practice for the design of such low transformation temperature (LTT) filler alloys are considered. By engineering the phase transformation temperature of the weld metal so as to take advantage of transformation expansion, the residual stress state within the weld zone can be significantly altered, most particularly where the weld thermally contracts with any movement of base parts constrained. To date, the technique has been shown to increase fatigue strength for some common weld geometries, which may enable engineering design codes to be favourably re-drafted where such LTT filler alloys are used.

---

**Keywords**

Welding, Residual stress, Martensite, Low transformation temperature weld metal.

## **1. Introduction**

Welding integrity is crucial to many important industrial processes; welded structures in building construction, mining equipment, ships, agricultural machinery, bridges and off-shore platforms are just a few examples. Besides the efficiency of the process, equipment and operational costs are low, making the process favourable compared to other methods of joining. On the completion of welding, due to thermal contraction and geometric construction, a pattern of compressive and tensile residual stresses will be present in and adjacent to the weld zone on cooling to room temperature. The presence of tensile residual stress is said to be the main reason why the fatigue strength of a welded joint does not increase by strengthening the base steel [1]. In this review, the theory, latest concepts and practice for the design of welding alloys capable of offsetting such tensile, residual stresses in weld zones, generated from thermal contraction are presented. Such 'smart' alloys are particularly beneficial in mitigating tensile residual stress for constrained welds.

## **2. Theoretical and experimental basis of LTT weld filler alloys**

### **2.1 Transformation under constraint**

The mechanism by which the austenite transforms on cooling can be described as being either reconstructive or displacive movement of iron atoms to another lattice configuration. With displacive transformation, there is a homogeneous deformation of the original crystal arrangement into a new structure, which does not involve the bonds being broken and subsequent re-arrangement of atoms as seen in reconstructive transformation to give allotriomorphic ferrite and/or pearlite. When cooling rate is rapid (e.g. most weld scenarios) or if the weld metal is heavily alloyed, the displacive transformation becomes prevalent where the resultant microstructure can be acicular ferrite, bainite or martensite. The microstructural characteristics of such phase transformations from the austenite phase are extensively reviewed [1-5], but most importantly, such transformation is always couple with tremendous shear and volume expansion.

For relatively large and heavy parts being welded, most base material flanking the weld will be constrained, thus thermal contraction on cooling and inhomogeneity of temperature distribution will induce residual stresses in the weld 'zone' (i.e. the weld and flanking heat-affected areas). In the usual

case of long, thin weld run(s) between two parts, the highest tensile residual stress magnitude will be unidirectional. In order to counter-act the thermal contraction during cooling from the austenite with volume expansion, the transformation temperature can be engineered. Such residual stress / temperature relationships is shown schematically in Figure 1a where the transformation start temperature is observed by the sudden decrease in stress, which can be attributed to the dilatation and shear strains that occur and compensate the accumulated thermal contraction.

Experimentally, this effect during welding can be clearly shown with constrained cooling tests, such as the Satoh test. The test involves a tensile test specimen, which heated so as to be fully austenitic which is then control cooled under unidirectional restraint. Some results [6-8] are shown in Figure 1b for different types of steel (martensitic, bainitic and austenitic, respectively). It can be seen that the fully austenitic steel has a near-linear thermal contraction slope, while those of the bainite and martensite transformation reflect the reduction in residual stress; however the beneficial offset in contraction strain is negated by the continued cooling to ambient after the transformation product has been exhausted. These observations led to the conclusion that the final stress state of a welded component is not only affected by transformation temperature, but it has the potential to be reduced by lowering the transformation temperature. Figure 1c shows the effect on stress in such a reduction in transformation temperature with two alloys (LTTE and Series B). It can be seen that the stress is being driven into compression or near zero stress at room temperature, compared to that of a conventional filler alloy (OK75.78) which has a tensile stress at room temperature after transformation at  $\sim 450$  °C.

The effect of the phase transformation temperature of various weld filler alloys, on the residual stress distribution within the weld zone, was investigated by both Wang et al.[9] and Murata et al.[10]. Murata et al.'s results (Figure 2) showed that once the transformation temperatures get sufficiently low, not only are tensile residual stresses reduced to zero, but compressive residual stresses can be generated with cooling to at room temperature. These reach a maximum when the transformation of the filler alloy occurs around 200 °C. Below that temperature, the transformation and associate volume expansion are not complete on cooling to ambient temperature thus not fully cancelling the tensile residual stresses from restrained contractive cooling. If the phase transformation is absence (e.g. if an austenitic, weld filler alloy is used), then the tensile stress is expected to increase progressively due to uninterrupted thermal contraction.

Although significant research in this area only started two decades ago, it has been known for a longer period that tensile residual stresses in weld zones can be reduced by the use of 9% Ni filler alloy with a  $M_s$  of 350 °C [11] and compressive residual stresses can be obtained when the transformation temperatures are even lower (e.g.  $M_s = 250$  °C), as observed in filler alloy for maraging steels [12, 13].

### **2.3 Unconstrained tests**

For a linear weld run, the magnitude of the residual stresses generated during cooling in longitudinal and transverse direction will differ (Figure 2) with transformation start temperature. This figure illustrates that difference, plus the resultant angular distortion, from flat weld test sample [10]. This was shown clearly where unconstrained plates were V-notched and welded along the complete plate lengths [14]; angular distortion was reduced 45% by using an alloy with a transformation temperature range of 350-422°C compared with one with a range of 400-802°C. Further, distortion was minimal when using a filler alloy with a transformation start temperature of between 250 and 300°C. Such differences were also found valid for multi-pass welding [15]. The simple experimentation clearly shows that the use of such novel, LTT weld filler alloys will not only reduce harmful tensile residual stresses in constrained weld zones, but also minimise the weld zone distortion.

### **2.4 Residual stress surveys of welded test samples.**

Techniques for measuring residual stress can be classified as destructive or non-destructive. Destructive techniques involve disruption of the residual stress from its state of equilibrium, generally by material removal to create a free surface, whilst local changes in strain or displacement are measured (e.g. hole drilling and the 'contour method') [16-19].

Advances in non-destructive, diffraction based techniques such as in synchrotron X-Ray diffraction and neutron diffraction in recent years has facilitated the study of the effect of phase transformation and residual stress in 3-dimensional detail without destroying the sample [8, 20, 21]. Both techniques are essentially using the lattice parameter as a strain gauge [22]. Figure 3 shows neutron diffraction surveys across test welds for the three filler alloys; one standard, two LTT. Their chemical compositions and some respective mechanical properties of the alloys are given in Tables 1 and 2, respectively. The works have provided an insight into stress generation and has further shown that the use of LTT alloys

would result in near-zero or compressive residual stresses over the cross section of the weld metal, whilst tensile residual stresses remain in the non-transformable HAZ (Heat Affected Zone). The measured tensile residual stresses in the HAZ are lower compared to those seen in welds where conventional, high transformation temperature, filler alloys have been used [8, 21]. This is due to the expansion force of the weld metal phase transformation that counteracts the tensile residual stress generated due to the contraction of non-transformable HAZ.

### 3.0 Design of LTT 'smart' weld filler alloys

The previous sections have shown the importance in lowering the phase transformation temperature in these LTT alloys to ensure maximal expansion to relieve tensile, residual stresses generated during thermal contraction. It is also importance to consider other design requirements during alloy design. The LTT alloy should have higher or equal strength compared to the base metal as well as appropriate toughness. Whilst design factors such as 'weldability' and susceptibility to hot and cold cracking should be considered when new weld alloys are designed, factors such as the corrosion resistance would depend upon the application of the alloy.

The temperature of phase transformation of the LTT alloy is strongly dependent on the content of the austenite ( $\gamma$ )-stabilizing alloying elements. The known and most commonly used  $\gamma$  -stabilizing alloying elements are carbon, nickel, manganese and chromium; these are discussed in detail in below. Various LTT alloys, which have been investigated by various researchers, are listed in Table 1 with respect to chemical composition,  $M_s$  temperature and expansion strain where given; in the following Table 2, mechanical properties are listed where given. All data are cross-referenced to respective sources within the tables.

Low carbon and nitrogen contents are very desirable for a filler weld alloy to prevent the formation of hard and brittle martensite in the HAZ, which is susceptible to hydrogen-assisted cold cracking. The lower limit of carbon content in weld alloy is normally reported being about 0.03 wt%; however if this value could be further lowered, to say 0.003 wt% (as obtained in an interstitial free steel), significant improvement of toughness would be expected. As shown in Table 2, the toughness of LTT weld metal 'B206' was significantly improved when the carbon content was reduced to 0.01 wt%.

With reference to Table 1, low carbon and nitrogen plus the addition of certain alloying elements are required lower the transformation temperature. Nickel can be a popular choice of alloying as it is known to improve toughness, when the cost of nickel is not too expensive. Francis et al.[21] and Darcis et al.[23] have designed a LTT alloy with nickel as a major alloying element; however its toughness was not significantly better than alloys with a chromium and nickel combination. A more cost effective alloying element is manganese and attempts has been made to design manganese based, weld filler alloys in which silicon has been added to improve the bead morphology; however their toughness has been low [24] Martensitic Fe-Mn alloys can be very brittle [25-29] probably as a result of a co-segregation of manganese and phosphorus to prior austenite grain boundaries [25, 27, 30].

Although chromium is a ferrite stabiliser, about 10-14 wt% can be added to decrease the transformation temperature. In this instance, the alloy can be easily designed to have a minimum of 12 wt% so that the alloy can be 'stainless'. Low carbon content is also required to prevent the formation of chromium carbides during the reheating process. Formation of such precipitates would result in inter-granular attack due to chromium depletion. Chromium additions also improve the oxidation resistance.

Most of the LTT alloys designed in the past two decades to date have had a combination of Cr and Ni with most also having a low carbon content [31-33]. The content of nickel has been adjusted to between 5 and 11 wt% to control the phase transformation starting temperature. This is considered to be the most economic option where reasonable toughness can be obtained. There was a concern of galvanic corrosion when these types of LLT alloy were used to weld high strength low alloy steel due to the compositional mismatch. However, work in Japan had shown no trace of selective/galvanic corrosion in synthetic sea water when LLT filler alloys were use to weld high strength low alloy steel [34]. Similar results were also obtained by Zenitani et al.[35].

Impurity elements like sulphur and phosphorus should be kept as low as possible whilst elements like molybdenum and tungsten can be added dependent upon whether the application, for example if pitting corrosion is to be prevented. Micro-alloying elements such as titanium and niobium can be used to control nitrogen content.

Considerable experience in stainless steel welding research has shown that alloys that solidify as primary ferrite are resistant to hot cracking compared with alloys that solidify entirely as austenite.

Therefore, it is also preferable to design 'smart' LTT alloys with primary ferrite solidification. Small amount of discontinuous  $\delta$  ferrite can be left in the weld with ferritic solidification as this is believed to be beneficial to toughness [36]. However, if there is a significant amount of  $\delta$  ferrite such that a continuous network forms, this has been found to be detrimental to impact toughness with a high ductile to brittle transition temperature [37]. The austenite grain size will also be finer where it is formed from the decomposition of  $\delta$ -ferrite compared with the grain size of austenite formed directly from the molten weld metal [38]. A fine grain size will also contribute to higher toughness.

It should be noted that the phase transformation temperature of the LTT filler alloy in actual welds, as against Satoh type test rigs, will be affected by other variables, such as dilution by the base metal, the high temperature cooling rate, which affects the amount of  $\delta$  ferrite formed, which in turn will affect the carbon content of the austenite.

#### **4.0 Calculation of the $M_s$ and martensite transformation**

It has been shown that the phase transformation temperature of the filler metal can significantly change the distribution of residual stress; therefore it can be very beneficial to determine an alloy composition which will give an advantageous transformation temperature together with a suitable transformed microstructure. When the phase transformation is depressed to very low temperature or when significant alloying elements are added, it is often the case that the martensite will form. The temperature of the martensite start temperature ( $M_s$ ) of the filler weld metal is strongly dependent on the content of austenite stabilizing alloying elements. The effect of the chemical composition on  $M_s$  temperature has been extensively researched over the years. Several linear regression empirical equations have been proposed [39-43] whilst thermodynamic [44-47] and artificial neural network models [48-50] were also developed to predict  $M_s$  temperatures. All such methods provide a reasonable guide during the design stage as long as they are used within the data boundaries stipulated by the respective model. This includes a thermodynamic model where its accuracy is limited by the underlying thermodynamic, empirically obtained, database [49].

The martensite reaction occurs athermally and is effectively not time dependent; the amount transformed is dependent on the degree of undercooling beneath the  $M_s$  temperature. This is expressed by the equation of Koistinen and Marburger [51]:

$$1 - V_{\alpha'} = V_{\gamma} = \exp\{-b(M_s - T_q)\} \text{ where } b \approx 1.10 \times 10^{-2} \text{K}^{-1} \quad [1]$$

where  $V_{\alpha'}$  is the fraction of martensite,  $V_{\gamma}$  the volume fraction of retained austenite and  $T_q$  the 'quenching' temperature below  $M_s$  to which the sample is cooled. Whilst a value of material constant  $b = 1.1 \times 10^{-2} \text{K}^{-1}$  is normally quoted for ferrous martensite [4], it has been determined that 'b' lies within the range,  $1.75\text{-}1.90 \times 10^{-2} \text{K}^{-1}$ , in low carbon, chromium and nickel rich welding alloys [52].

## **5.0 Applications of LTT 'smart' alloys**

### **5.1 Application of LTT 'smart' alloys to improve fatigue strength**

In comparison with its static strength, the fatigue strength of a joint welded using a conventional filler alloy is much weaker. As shown in Figure 4, welded components have a comparatively low fatigue resistance. Although the fatigue strength of the base metal will increase with increasing base metal yield strength, the fatigue strength for a particular welded component remains more or less constant, despite weld dilution. This is why the fatigue tolerances for welded structures in the design code are classified into joint type according to the type of weld and its orientation with respect to the applied fluctuating loads rather than being based on the yield strength of the base materials [53].

The low fatigue resistance of the welded joint is mainly due to a short crack initiation period. This is significantly influenced by the joint geometry and also the tensile residual stress distribution in the joint weld zone. The former can include the abrupt shape change and/or a surface defect that induces stress concentration.[54] The sharper the transition between the weld bead and the parent material, the higher the stress concentration will be and thus the greater effect on fatigue life. The introduction of tensile residual stresses not only reduces the fatigue crack initiation resistance and the fatigue limit of the welded components,[55] but also increases the fatigue crack growth rate [9, 56].

It is possible to apply post weld treatments to improve the fatigue performance and significant work has been done to extend the crack initiation life of welded joints. In general, the post weld improvement methods can be classified into weld geometry improvement and residual stress alteration. The weld geometry can be improved by, for example, TIG-dressing [57, 58] or grinding to reduce the

stress concentration factor. However, in fillet welds, it is not always possible to eliminate the geometrical effect. The second approach is to alter the residual stress present, either by mechanical or thermal means. It can be the introduction of surface compressive stresses by locally deforming the surface e.g. shot-peening or hammering etc. [59, 60] or by post-weld heat treatment [61] to relieve the residual stresses. While all of these techniques are efficient in increasing fatigue life, these processes also required additional work after welding, which are both time consuming and an additional cost [62, 63].

LTT welding facilitates not only the reduction of tensile residual stresses, particularly transversely across the weld zone, but also the generation of compressive residual stresses in the weld zone, thus increasing fatigue strength. Such improvements have been found for all types of welded joint [31, 33, 64-70]. This achievement is based entirely on the fact that the reduction of the transformation temperature allows the volume expansion originated from martensite transformation to compensate for the accumulated thermal contraction strains, with that expansion variant directional when the weld cools within a directional, non-hydrostatic, stress field. Early work has also shown that the fatigue strength of a non-load-carrying cruciform welded joint increases in proportion to the increased base metal strength when LTT welding wire alloy is used [71, 72]. A further benefit in using LTT filler alloys has been found where there are weld surface defects, such as blowholes. It has been claimed that blowholes of about 4.5 mm diameter in a LTT weld were found to have not reduced fatigue strength, as the compressive residual stress around them prevented the fatigue crack initiation by the stress ratio effect [65].

Cruciform joints [23] and out-of-plane gusset (box) welded joints [73, 74] have, to date, been the most common test geometry in fatigue strength investigations of the LTT weld filler alloy effect. As is shown in Figure 5, that these types of joint generally a comparatively low fatigue strength and there is an obvious cost and design benefit if their fatigue strengths can be improved by using such filler alloys.

The LTT welds have shown a considerable improvement of fatigue resistance compared to that of conventional joints in constant amplitude fatigue testing, with some reports showing about 40% increase in mean fatigue strength [23, 31, 64, 66, 68, 75]. However with variable amplitude fatigue testing, the improvement observed was not as significant (12%) compared with that found during

constant amplitude loading [75]. This was mainly due to the relaxation of the compressive residual stresses at high amplitude loading during variable amplitude fatigue.

### **5.3 Welding processes suitable for use of LTT 'smart' alloys**

As discussed in the previous section, very low carbon and nitrogen are paramount to obtain good toughness and this can be obtained readily with metal-cored wires [37]. The wires are suitable for submerged arc (SAW), tungsten inert gas (TIG) and metal inert/active gas (MIG/MAG) welding, offering the requisite versatility and high output. When MIG/MAG is chosen, a gas mixture containing a high proportion of carbon dioxide must be prohibited since this will lead to an increase in carbon content of the deposited metal. Another significant effect on toughness is oxygen content, which varies with respective welding processes. As shown in Figure 6, the toughness of martensitic steel welds decrease with increasing oxygen contamination [37, 76-78]. It also shows that TIG process produce the lowest oxygen content compare to other process. Excessive inclusion formation and significant loss of alloying elements to the slag are the main reason why the mechanical properties of weld metal are diminished by high oxygen content.

### **5.4 Effect of inter-pass temperature on multi-pass LTT alloy welds**

The interpass temperature was found significant, as distinctly different residual stress fields were obtained with different interpass temperatures. If interpass temperatures are higher than the martensite start temperature ( $M_s$ ) thus giving an austenitic matrix, all passes will only transform into martensite after respective welding runs are completed. Therefore, much of the fusion zone will be left under compressive stress. Where interpass temperatures are lower, with underlying pass temperatures not exceeding the  $M_s$  temperature, the underlying weld runs zones will be tempered rather than re-austenitized. As a consequence, only a small zone around or within the final weld run will be in compressive stress, while other regions will have tensile residual stress zones [79].

### **5.5 Effect of post-weld treatment where LTT weld filler alloy has been used**

Thibault et al.[79] have characterized residual stress patterns on LTT weld that had undergone a standardized post-weld heat treatment. They showed that post weld heat treatment not only reduced the

harmful tensile residual generated in non-transformable HAZ, but also generated beneficial compressive stresses.

### **5.6 Effect of welded geometry and dilution**

These have also been found to affect significantly the  $M_s$  temperature [80, 81]. The optimum  $M_s$  temperature of the weld filler metal required for the introduction of residual compressive stress and minimum distortion in a butt weld is  $\sim 200^\circ\text{C}$ , whereas for a fillet welded T joint, optimum  $M_s$  is  $\sim 400^\circ\text{C}$ , where the transient angular distortion is minimised. Recent work by authors have shown that dilution must be considered when using LTT filler alloys for welding austenitic stainless steels, which may have higher alloying concentrations than the welding alloy. Such concentrations may lower the  $M_s$  temperature such that significant transformation may not occur. It has been shown that after a first pass the microstructure can remain austenitic, whereas with subsequent passes there was transformation to martensitic. This shows that different configuration shape of the welded joint, or structural restraint, as well as welding conditions all influence the residual stress pattern generated.

Heavily alloy weld metal has been produced to counter the dilution effect [70]. It is found that the element concentration of welds was significantly lower than the initial pure alloy material with dilution levels varying between  $\sim 25\text{--}35\%$  for single-pass and  $\sim 10\%$  for two-pass welds [70]. The work highlights that single pass dilution effects and the improvements in fatigue performance that can be achieved. The dilution effect on fatigue was considered to be a result of the  $M_s$  change influencing residual stress rather than microstructure.

### **5.7 Cold cracking resistance in LTT 'smart' alloys**

Whilst it has been shown that the use of LTT weld alloys is effective in the mitigation of harmful residual stresses, the martensitic microstructure of some LTT alloys can be susceptible to cold cracking. Zenitani et al. [82, 83] and Kromm et al. [84] have investigated the cold cracking behaviour of LTT weld alloys using the Tekken test. They found that LTT weld metals with a two phase microstructure (martensite and retained austenite) had excellent cold cracking resistance where the  $M_s$  temperature is even lower than normal for LTT alloys and where some retained austenite was still

present at room temperature. Such retained austenite facilitated hydrogen entrapment hence reducing cold cracking susceptibility.

## **6.0 Finite Element Modelling**

Whilst the residual stresses would be generated from uneven heat dissipation and any restrictions on expansion and contraction within localised areas, their magnitude would vary dependent upon the joint restraint, its geometry and the specific welding process employed. If the parts to be joined were free to expand and contract then the residual stresses would be minimal. Where the heat input range varies with different welding processes, the residual stresses generated will differ [77]. The material's physical and mechanical properties, that affect the type and magnitude of residual stress will include the heat capacity, thermal expansion coefficient, density and strength. Poor thermal conductivity and high thermal expansion coefficient would increase significantly the residual stresses in a weldment, for example, austenitic stainless steel.

Given the complexity of the physical processes that are taking place, it would be of great benefit to know whether a weld zone residual stress distribution could be predicted on the basis of the weld filler alloy transformation behaviour. To this end, numerous finite element software packages [85, 86] were created to account all aspects of the respective welding processes; these included heat flow, material behaviour and evolution of stress and strain. These newly developed models also accounted for transformation plasticity [87, 88]. While the welding condition and material properties inputs are straight forward, it has been reported that finite element simulation has shown that the transformation temperature of the weld metal does not have a significant effect on the magnitude of the peak stresses beyond the HAZ and that this is due to the unaccounted variant selection during simulation [20]. In this respect, it was suggested that variant selection must be incorporated in the simulation in order to more accurately predict the weld zone residual stress distributions where LTT weld filler alloys have been used.

## **6. Conclusions**

The steady cooling curve for the residual stress - temperature relationship for the contraction of steel weld zone on cooling is interrupted by the period of expansion due to crystallographic phase

transformation on cooling from austenite. Where transformation is completed well above room temperature, the transformed product will then further contract introducing the tensile residual stress. The lower the transformation temperature, the less the effect of this. If full transformation occurs near room temperature, for some situations around 200 °C, then the benefit of transformation expansion can be exploited to greatly reduce critical concentrations of any harmful tensile residual stresses and, with some alloys, even generate beneficial, compressive residual stresses within the weld zone. Such improvements apply to multi-pass welds as well as single pass welds, although the magnitude of the effect is dependent upon re-heat temperatures of previous passes.

Reducing harmful tensile residual stress concentrations or even generating compressive residual stresses in weld zones will give increased resistance to fatigue. This in turn, may require design codes to be reviewed where LTT filler alloys are used. Additionally, proscribed post weld heat treatments may not be required.

Further research and development into suitable LTT alloys should continue and be expanded to quantify their beneficial affects with different weld configurations, particularly on-site, with different weld environments and base steels.

### **Acknowledgements**

Prof. H.K.D.H. Bhadeshia and the Department of Metallurgy and Materials of the University of Cambridge, UK, for Project initiation, help and support. The author would also like to thank MOD and ESAB for funding.

### **References**

- [1] Bhadeshia HKDH. Material Factors. In. Handbook of Residual Stress and Deformation of Steel, Totten G, Howes M, Inoue T. editors. Ohio: ASM International; 2002. p. 3-10.
- [2] Bhadeshia HKDH. Some phase transformations in steels. Mater Sci Technol. 1999;15:22-9.
- [3] Bhadeshia HKDH. Phase transformations contributing to the properties of modern steels. Bulletin of the Polish Academy of Sciences: Technical Sciences. 2010;58:255-65.

- [4] Bhadeshia HKDH, Honeycombe RWK. Steels : Microstructure and Properties. 3rd ed. / Harry Bhadeshia, Robert Honeycombe. ed. Oxford: Butterworth-Heinemann; 2006.
- [5] Krauss G. Microstructure and transformations in steels. In. Materials Science & Technology: A Comprehensive Treatment, Microstructure and Transformation in Steel, Pickering FB.Editors. Weinheim, New York, Cambridge: VCH; 1992. p. 13.
- [6] Jones WKC, Alberry PJ. A model for stress accumulation in steels during welding. In:Residual stress in welded construction and their effects, Nichols RW, London, The Welding Institute, 1977.
- [7] Bhadeshia HKDH. Possible effects of stress on steel weld microstructure. Mathematical Modelling of Weld Phenomena. 1995:71-118.
- [8] Francis JA, Stone HJ, Kundu S, Rogge RB, Bhadeshia HKDH, Withers PJ, et al. Transformation Temperatures and Welding Residual Stresses in Ferritic Steels. In:Proceedings of PVP2007, ASME Pressure Vessels and Piping Division Conference, San Antonio, Texas, 2007.
- [9] Wang W, Huo L, Zhang Y, Wang D, Jing H. New developed welding electrode for improving the fatigue strength of welded joints. Journal of Materials Science And Technology. 2002;18:527-31.
- [10] Murata H, Kato N, Tamura H. Effect of transformation on residual stress in welding. Yosetsu Gakkai Ronbunshu/Quarterly Journal of the Japan Welding Society. 1993;11:545-50.
- [11] Satoh K, Matsui S, Machida T. Thermal Stresses Developed In High-strength Steels Subjected To Thermal Cycles Simulating Weld Heat-affected Zone. Journal of the Japan Welding Society. 1966;35:780-9.
- [12] Lang FH, Kenyon N. Welding of maraging steels. Welding Research Council Bulletin. 1971.
- [13] Luxmoore A, Kan DKY, Egan GR. Residual Stresses In Welded Maraging Steel Sheet. Residual stresses in welded maraging steel sheet (Residual stresses near weld in spherical rocket motor casing constructed from maraging steel sheet, discussing moire measurement and reduction treatments). 1970;2:229-34.
- [14] Bhadeshia HKDH. Developments in martensitic and bainitic steels: Role of the shape deformation. Materials Science and Engineering A. 2004;378:34-9.
- [15] Murata H, Tamura H, Kato N, Shiramatu O. Effect of transformation temperature on angular distortion. Yosetsu Gakkai Ronbunshu/Quarterly Journal of the Japan Welding Society. 1993;11:173-9.
- [16] Bahadur A, Kumar BR, Kumar AS, Sarkar GG, Rao JS. Development and comparison of residual stress measurement on welds by various methods. Materials Science and Technology. 2004;20:261-9.

- [17] Cho JR, Lee BY, Moon YH, Van Tyne CJ. Investigation of residual stress and post weld heat treatment of multi-pass welds by finite element method and experiments. *Journal of Materials Processing Technology*. 2004;155-156:1690-5.
- [18] Thibault D, Bocher P, Thomas M. Residual stress and microstructure in welds of 13%Cr-4%Ni martensitic stainless steel. *Journal of Materials Processing Technology*. 2009;209:2195-202.
- [19] Zhang Y, Ganguly S, Edwards L, Fitzpatrick ME. Cross-sectional mapping of residual stresses in a VPPA weld using the contour method. *Acta Materialia*. 2004;52:5225-32.
- [20] Dai H, Francis JA, Stone HJ, Bhadeshia HKDH, Withers PJ. Characterizing Phase Transformations and Their Effects on Ferritic Weld Residual Stresses with X-Rays and Neutrons. *Metallurgical and Materials Transactions A*. 2008;39:3070-8.
- [21] Francis JA, Stone HJ, Kundu S, Bhadeshia HKDH, Rogge RB, Withers PJ, et al. The Effects of Filler Metal Transformation Temperature on Residual Stresses in a High Strength Steel Weld. *Journal of pressure vessel technology*. 2009;131.
- [22] James MR, Lu J. Handbook of measurement of residual stresses. In. Society for Experimental Mechanics, Lu J: Fairmont Press; 1996.
- [23] Darcis PP, Katsumoto H, Payares-Asprino MC, Liu S, Siewert TA. Cruciform fillet welded joint fatigue strength improvements by weld metal phase transformations. *Fatigue and Fracture of Eng Mater and Structures*. 2008;31:125-36.
- [24] Martínez Díez F, Liu S. Development of compressive residual stress in structural steel weld toes by means of weld metal phase transformations. In:ASM Proceedings of the International Conference: Trends in Welding Research, David SA, DebRoy T, DuPont JN, Koseki T, Smartt HB, Georgia, USA, ASM International, 2005.
- [25] Bolton JD, Petty ER, Allen GB. The mechanical properties of  $\alpha$ -phase low carbon Fe-Mn alloys. *Metallurgical Transactions*. 1971;2:2915-23.
- [26] Holden A, Bolton JD, Petty ER. Structure and properties of iron manganese alloys. *Journal of the Iron and Steel Institute*. 1971:721-8.
- [27] Edwards BC, Nasim M, Wilson EA. The nature of intergranular embrittlement in quenched FeMn alloys. *Scripta Metallurgica*. 1978;12:377-80.
- [28] Gulyaev AP, Volynova TF. Brittleness of  $\alpha$ ,  $\epsilon$ , and  $\gamma$  solid solutions of Fe-Mn alloys. *Met Sci Heat Treat*. 1979;21:98-104.
- [29] Yasushi K. Embrittling behavior in high manganese martensitic steels. *Tetsu-to-Hagane : Journal of the Iron & Steel Institute of Japan*. 1985;71:S1465

- [30] de Souza LFG, de Souza Bott I, Jorge JCF, Guimarães AS, Paranhos RPR. Microstructural analysis of a single pass 2.25%Cr - 1.0%Mo steel weld metal with different manganese contents. *Materials Characterization*. 2005;55:19-27.
- [31] Ohta A, Suzuki N, Maeda Y, Hiraoka K, Nakamura T. Superior fatigue crack growth properties in newly developed weld metal. *Int J Fatigue*. 1999;21:S113-S118.
- [32] Zenitani S, Hayakawa N, Yamamoto J, Hiraoka K, Morikage Y, Kubo T, et al. Development of new low transformation-temperature welding consumable to prevent cold cracking in high strength steel welds. *Yosetsu Gakkai Ronbunshu/Quarterly Journal of the Japan Welding Society*. 2005;23:95-102.
- [33] Lixing H, Dongpo W, Wenxian W, Yufeng Z. Ultrasonic peening and low transformation temperature electrodes used for improving the fatigue strength of welded joints. *Welding in the World*. 2004;48:34-9.
- [34] Ohta A, Maeda Y, Suzuki N, Watanabe O, Kubo T, Katsuoka K. Fatigue strength improvement of box welds using low transformation temperature welding material. Tripled fatigue strength by post weld heat treatment. *Welding International*. 2002;16:44 - 7.
- [35] Zenitani S, Nishimura T, Hayakawa N, Hiraoka K. Atmospheric corrosion behavior of high strength steel weld joints formed by low transformation-temperature welding consumables. *Yosetsu Gakkai Ronbunshu/Quarterly Journal of the Japan Welding Society*. 2006;24:291-8.
- [36] Shirzadi AA, Bhadeshia HKDH, Karlsson L, Withers PJ. Stainless steel weld metal designed to mitigate residual stresses. *Sci and Technol of Welding and Joining*. 2009;14:559-65.
- [37] Karlsson L, Rigdal S, Bruins W, Goldschmitz M. Development of matching composition supermartensitic stainless steel welding consumables. *Svetsaren, A Welding Review*. 1999;54:3-7.
- [38] Zhang Z, Farrar RA. Columnar grain development in C-Mn-Ni low-alloy weld metals and the influence of nickel. *J Mater Sci*. 1995;30:5581-8.
- [39] Wang J, Van Der Wolk PJ, Van Der Zwaag S. Determination of martensite start temperature in engineering steels. Part I. Empirical relations describing the effect of steel chemistry. *Materials Transactions, JIM*. 2000;41:761-8.
- [40] Grange RA, Stewart HM. The Temperature Range of Martensite Formation. *Transactions of the American Institute of Mining and Metallurgical Engineers*. 1946;167:467-501.
- [41] Payson P, Savage CH. Martensite Reactions in Alloy Steels. *Transactions of the American Society of Metals*. 1944;33:261-80.

- [42] Andrews KW. Empirical formulae for the calculation of some transformation temperatures. The Journal of the Iron and Steel Institute. 1965;203:721-7.
- [43] Steven W, Haynes AG. The temperature of formation of martensite and bainite in low-alloy steels. The Journal of the Iron and Steel Institute. 1956;183:349-59.
- [44] Ghosh G, Olson GB. Kinetics of F.C.C. → B.C.C. heterogeneous martensitic nucleation--I. The critical driving force for athermal nucleation. Acta Metall Mater. 1994;42:3361-70.
- [45] Ghosh G, Olson GB. Kinetics of F.C.C. → B.C.C. heterogeneous martensitic nucleation--II. Thermal activation. Acta Metall Mater. 1994;42:3371-9.
- [46] Bhadeshia HKDH. Thermodynamic extrapolation and martensite-start temperature of substitutionally alloyed steels. Met Sci. 1981;15:178-80.
- [47] Cool T, Bhadeshia HKDH. Prediction of martensite start temperature of power plant steels. Mater Sci Technol. 1996;12:40-4.
- [48] Capdevila C, Caballero FG, de Andres CG. Analysis of effect of alloying elements on martensite start temperature of steels. Mater Sci Technol. 2003;19:581-6.
- [49] Sourmail T, Garcia-Mateo C. Critical assessment of models for predicting the Ms temperature of steels. Comp Mater Sci. 2005;34:323-34.
- [50] Vermeulen WG, Morris PF, De Weijer AP, Van der Zwaag S. Prediction of martensite start temperature using artificial neural networks. Ironmaking and Steelmaking. 1996;23:433-7.
- [51] Koistinen DP, Marburger RE. A general equation prescribing the extent of the austenite-martensite transformation in pure iron-carbon alloys and plain carbon steels. Acta Metall. 1959;7:59-60.
- [52] Yamamoto J, Meguro S, Muramatsu Y, Hayakawa N, Hiraoka K. Analysis of martensite transformation behavior in welded joint of low transformation-temperature materials. Yosetsu Gakkai Ronbunshu/Quarterly Journal of the Japan Welding Society. 2007;25:560-8.
- [53] Gurney TR. A comparison of fatigue design rules. In: Proceedings of the Conference on Fatigue of Welded Structures, Gurney TR, Brighton, The Welding Institute, 1970.
- [54] Maddox SJ. Fatigue Strength of Welded Structures. Cambridge: Abington Publishing; 1991.
- [55] Jang C, Cho PY, Kim M, Oh SJ, Yang JS. Effects of microstructure and residual stress on fatigue crack growth of stainless steel narrow gap welds. Materials and Design. 2010, 31:1862-70.
- [56] Ohta A, Suzuki N, Maeda Y. Unique fatigue threshold and growth properties of welded joints in a tensile residual stress field. Int J Fatigue. 1997;19:303-10.
- [57] Huo L, Wang D, Zhang Y. Investigation of the fatigue behaviour of the welded joints treated by TIG dressing and ultrasonic peening under variable-amplitude load. Int J Fatigue. 2005;27:95-101.

- [58] Dahle T. Design fatigue strength of TIG-dressed welded joints in high-strength steels subjected to spectrum loading. *Int J Fatigue*. 1998;20:677-81.
- [59] Habibi N, H-Gangaraj SM, Farrahi GH, Majzoubi GH, Mahmoudi AH, Daghigh M, et al. The effect of shot peening on fatigue life of welded tubular joint in offshore structure. *Materials & Design*. 2012;36:250-7.
- [60] Abdullah A, Malaki M, Eskandari A. Strength enhancement of the welded structures by ultrasonic peening. *Materials & Design*. 2012;38:7-18.
- [61] Ravi S, Balasubramanian V, Babu S, Nasser SN. Assessment of some factors influencing the fatigue life of strength mis-matched HSLA steel weldments. *Materials & Design*. 2004;25:125-35.
- [62] Masubuchi K. Residual Stress and Distortion. In. *ASM Handbook Welding, Brazing & Soldering*, Davis JR. editors. Metals Park, Ohio: American Society for Metals; 1993. p. 856.
- [63] Zinn W, Scholtes B. Residual stress formation processes during welding and joining. *Handbook of Residual Stress and Deformation of Steel*. 2002:391-6.
- [64] Eckerlid J, Nilsson T, Karlsson L. Fatigue properties of longitudinal attachments welded using low transformation temperature filler. *Sci and Technol of Welding and Joining*. 2003;8:353-9.
- [65] Ohta A, Maeda Y, Nguyen NT, Suzuki N. Fatigue strength improvement of box section beam by low transformation temperature welding wire. *Welding in the World*. 2000;44:26-30.
- [66] Ohta A, Suzuki N, Maeda Y, Maddox SJ. Fatigue strength improvement of lap welded joints by low transformation temperature welding wire - Superior improvement with strength of steel. *Welding in the World, Le Soudage Dans Le Monde*. 2003;47:38-43.
- [67] Ohta A, Watanabe O, Matsuoka K, Siga C, Nishijima S, Maeda Y, et al. Fatigue strength improvement of box welded joints by using low transformation temperature welding material. *Yosetsu Gakkai Ronbunshu/Quarterly Journal of the Japan Welding Society*. 2000;18:141-5.
- [68] Karlsson L. Improving fatigue life with low temperature transformation (LTT) welding consumables. *Svetsaren*. 2009;64:27-31.
- [69] Karlsson L, Mráz L, Bhadeshia HKDH, Shirzadi AA. Comparison of alloying concepts for Low Transformation Temperature (LTT) welding consumables. *Biuletyn Instytutu Spawalnictwa*. 2010;54:33-9.
- [70] XV ESAB welding Seminar: Increasing fatigue life with low transformation temperature (LTT) welding consumables. Place, April 2011.
- [71] Fumimaru K, Kazuyuki M, Tadashi O, Tsutomu K, Masahiro T, Takahiro K. Steel Plates for Bridge Use and Their Application Technologies. *JFE TECHNICAL REPORT*. 2004;2:85-90.

- [72] Morikage Y, Kubo T, Yasuda K, Amano K, Hiraoka K, Ohta A, et al. Effect of Steel Strength on Fatigue Strength of Welded Joints Using Low-Temperature Transformation Welding Consumables. Pre-Prints of the National Meeting of JWS. 2001;68:144-1456.
- [73] Ohta A, Watanabe O, Matsuoka K, Maeda Y, Suzuki N, Kubo T. Fatigue strength improvement of box welds by low transformation temperature welding wire and PWHT. *Welding in the World*. 2000;44:52-6.
- [74] Ohta A, Watanabe O, Matsuoka K, Siga C, Nishijima S, Maeda Y, et al. Fatigue strength improvement by using newly developed low transformation temperature welding material. *Welding in the World*. 1999;43:38-42.
- [75] Barsoum Z, Gustafson M. Spectrum fatigue of high strength steel joints welded with low temperature transformation consumables. In:2nd International Conference on Fatigue Design, Senlis, France, 2007.
- [76] Nakamura S, Hasegawa T, Shimura R, Kimoto I. Effect of oxygen content on toughness in high strength weld metal. *Materials Science Forum*. 2010, p. 3687-92.
- [77] Kou S. *Welding metallurgy*. 2nd ed. New York: John Wiley & Sons; 2003.
- [78] Terashima S, Bhadeshia HKDH. Changes in toughness at low oxygen concentrations in steel weld metals. *Sci and Technol of Welding and Joining*. 2006;11:509-16.
- [79] Thibault D, Bocher P, Thomas M, Gharghoury M, Côté M. Residual stress characterization in low transformation temperature 13%Cr-4%Ni stainless steel weld by neutron diffraction and the contour method. *Materials Science and Engineering A*. 2010;527:6205-10.
- [80] Mikami Y, Morikage Y, Mochizuki M, Toyoda M. Angular distortion of fillet welded T joint using low transformation temperature welding wire. *Science and Technology of Welding and Joining*. 2009;14:97-105.
- [81] Nakashima Y, Kumon Y, Inose K, Nakanishi Y, Morikage Y, Kubo T, et al. Welding Distortion Behavior of Steel Welds with Low-temperature Transformation Welding Wire. IIW-Doc XV-1196-05. 2005.
- [82] Zenitani S, Hayakawa N, Yamamoto J, Hiraoka K, Shiga C, Morikage Y, et al. Prevention of Cold Cracking in High Strength Steel Welds by Applying Newly Developed Low Transformation-Temperature Welding Consumables. In:ASM Proceedings of the International Conference: Trends in Welding Research, 2002.

- [83] Zenitani S, Hayakawa N, Yamamoto J, Hiraoka K, Morikage Y, Kubo T, et al. Development of new low transformation temperature welding consumable to prevent cold cracking in high strength steel welds. *Sci and Technol of Welding and Joining*. 2007;12:516-22.
- [84] Kromm A, Kannengiesser T. Characterising Phase Transformations of Different LTT Alloys and their Effect on Residual Stresses and Cold Cracking. *Welding in the world*. 2001;55:48-56.
- [85] Bergheau JM, Leblond JB. Coupling between heat flow, metallurgy and stress-strain computations in steels-The approach developed in the computer code SYSWELD for welding or quenching. *Modeling of Casting, Welding and Advanced Solidification Processes V*. 1991:203-10.
- [86] User Manual for UMAT-CAT - A Welding Specific User Material Routine Interfaced with ABAQUS, Version 3.1. 1999.
- [87] Wu T, Coret M, Combescure A. Numerical simulation of welding induced damage and residual stress of martensitic steel 15-5PH. *International Journal of Solids and Structures*. 2008;45:4973-89.
- [88] Liu C, Yao Kf, Liu Z, Gao G. Study of the effects of stress and strain on martensite transformation: Kinetics and transformation plasticity. *Journal of Computer-Aided Materials Design*. 2000;7:63-9.
- [89] Barsoum Z, Gustafsson M. Fatigue of high strength steel joints welded with low temperature transformation consumables. *Engineering Failure Analysis*. 2009;16:2186-94.
- [90] Payares-Asprino MC, Katsumoto H, Liu S. Effect of martensite start and finish temperature on residual stress development in structural steel welds. *Welding J*. 2008;87.
- [91] Murakawa H, Béréš M, Davies CM, Rashed S, Vega A, Tsunori M, et al. Effect of low transformation temperature weld filler metal on welding residual stress. *Sci and Technol of Welding and Joining*. 2010;15:393-9.
- [92] Miki C, Anami K. Improving Fatigue Strength by Additional Welding with Low Temperature Transformation Welding Electrodes. *Steel Structure*. 2001;1:25-32.
- [93] Kromm A, Kannengiesser T, Gibmeier J, Genzel C, Van Der Mee V. Determination of residual stresses in Low Transformation Temperature (LTT) weld metals using X-ray and high energy synchrotron radiation. *Welding in the World*. 2009;53:3-16.
- [94] Kromm A, Kannengiesser T, Gibmeier J. In-situ observation of phase transformations during welding of low transformation temperature filler material. *Materials Science Forum* 2010. p. 3769-74.
- [95] Yamamoto J, Meguro S, Muramatsu Y, Hayakawa N, Hiraoka K. Analysis of martensite transformation behaviour in welded joints of low transformation-temperature materials. *Welding International*. 2009;23:411-21.

- [96] Suzuki N, Ohta A, Maeda Y. Repair of fatigue cracks initiated around box welds by using low-transformation temperature welding material. *Yosetsu Gakkai Ronbunshu/Quarterly Journal of the Japan Welding Society*. 2003;21:62-7.
- [97] Kundu S. *Transformation Strain and Crystallographic Texture in Steels* Cambridge: University of Cambridge; 2007.
- [98] Maddox SJ. Fatigue design rules for welded structures. *Progress in Structural Engineering and Materials*. 2000;2:102-9.
- [99] Moat RJ, Stone HJ, Shirzadi AA, Francis JA, Kundu S, Mark AF, et al. Design of weld fillers for mitigation of residual stresses in ferritic and austenitic steel welds. *Sci and Technol of Welding and Joining*. 2011;16:279-84.
- [100] Yamamoto J, Hiraoka K, Mochizuki M. Analysis of martensite transformation behaviour in welded joint using low transformation temperature welding wire. *Sci and Technol of Welding and Joining*. 2010;15:104-10.
- [101] Wang W, Huo L, Zhang Y, Wang D. Investigation on phase stress and its application to improving fatigue strength of welded joints. *Jixie Gongcheng Xuebao/Chinese Journal of Mechanical Engineering*. 2002;38:65-8.
- [102] Bhadeshia HKDH, Francis JA, Stone HJ, Kundu S, Rogge RB, Withers PJ, et al. Transformation Plasticity in Steel Weld Metals. 10th International Aachen Welding Conference. 2007:171-9.

## List of Tables

Table 1: Chemical composition (wt.%),  $M_s$  temperature and expansion strain of LTT weld metals from various sources [8-10, 23, 31, 33, 64, 79, 82-84, 89-95]. Also included in the table are the chemical composition of the standard weld metals and base metal used in this review.

Table 2: Mechanical properties of LTT weld metals from various sources [21, 23, 64, 66, 92, 96].

## List of Figures

Fig. 1. Effect on residual stress with cooling; the balance of phase transformation expansion and thermal contraction.

(a) Stress temperature schematic (after [6]).

(Note - Thermal expansion coefficients for ferrite,  $13 \times 10^{-6} \text{K}^{-1}$ ; for austenite  $21 \times 10^{-6} \text{K}^{-1}$  [97]).

(b) Satoh test results for final residual stress of different steel phase types on cooling (after [6]).

(c) Satoh test results for conventional (OK75.78) and LTT weld filler alloys (LTTE & Series B). Samples had cooled from  $850^\circ\text{C}$  at  $10^\circ\text{C s}^{-1}$  (after [8]). Respective chemical composition data estimated transformation start temperatures and properties are shown in Tables 1 and 2.

Fig. 2. Directional differences in residual stress and angular distortion on cooling a test weld down to room temperature. (a) Relation between residual stress ( $\sigma_x$ ,  $\sigma_y$ ) of weld metal and starting temperature of transformation [10]. Similar results were also obtained by [9]. (b) Relation between total angular distortion after the final pass and the measured transformation starting temperature [10].

Fig. 3. Axial residual stress map (MPa) across HAZ's of welds using conventional filler alloy ('OK 75.78') and two LTT alloys ('LTTE', 'Series B'). (Their compositions, physical and cooling-residual stress properties are shown in Tables 1 & 2 and Figure 2c). Stresses were determined by neutron diffraction and superimposed on macrographs; stresses were averaged around the centre lines; i.e. "mirrored" (taken from reference [8]).

Fig. 4. Fatigue results [70] for single-pass fillet welds using a conventional filler alloy ('OK Autorod 89') and two LTT alloys ('LTT- C', 'LTT- S'). LTT-S provides evidence for improved fatigue

performance through designing an alloy to account for dilution. Open symbols represent specimens that did not fracture. Chemical compositions and Ms temperatures are given in Table 1.

Fig. 5. Effect of base metal test piece configuration on welded component fatigue life [67, 98].

Fig 6. Influence of oxygen content on Charpy-V toughness at -20°C and -40°C in Mo-alloyed supermartensitic weld metal [37].

**Table 1:** Chemical composition (wt.%),  $M_s$  temperature and expansion strain of LTT weld metals from various sources [8-10, 23, 31, 33, 64, 79, 82-84, 89-95]. Also included in the table are the chemical composition of the standard weld metals and base metal used in this review.

| LTT alloy identification | C     | Si       | Mn   | Cr    | Ni    | Mo    | Other   | $M_s$ (°C) | Expansion Strain (%) | Ref.      |
|--------------------------|-------|----------|------|-------|-------|-------|---------|------------|----------------------|-----------|
| 10Cr-10Ni                | 0.025 | 0.32     | 0.7  | 10    | 10    | 0.13  |         | 180        | 0.55                 | [31, 74]  |
| L2                       | 0.04  | 0.17     | 0.27 | 11.69 | 10.01 | 0.04  |         | 80         | 0.28                 | [9]       |
| L3                       | 0.04  | 0.17     | 0.3  | 10.51 | 9.62  | 0.05  |         | 138        | 0.52                 |           |
| L4                       | 0.07  | 0.230.23 | 1.25 | 9.1   | 8.46  | 0.05  |         | 191        | 0.63                 |           |
| L5                       | 0.08  | 0.230.17 | 1.35 | 7.78  | 6.88  | 0.06  |         | 242        | 0.54                 |           |
| L6                       | 0.07  | 0.23     | 1.3  | 6.3   | 5.29  | 0.04  |         | 287        | 0.48                 |           |
| L7                       | 0.09  | 0.47     | 1.51 | 5.07  | 4.43  | 0.06  |         | 325        | 0.44                 |           |
| L8                       | 0.08  | 0.45     | 1.5  | 3.91  | 3.23  | 0.04  |         | 408        | 0.36                 |           |
| LTTE                     | 0.07  | 0.2      | 1.3  | 9.1   | 8.5   |       |         | 200        |                      |           |
| Series B                 | 0.03  | 0.65     | 0.5  | 1     | 12    | 0.5   |         | 275        |                      |           |
| B206/ OK Tubrod 15.55    | 0.01  | 0.4      | 1.1  | 12.5  | 6.7   | 2.5   | 0.5Cu   |            |                      | [64, 89]  |
| 13Cr/LC35                | 0.04  | 0.5      | 0.8  | 12.3  | 7.3   | 2.2   |         |            |                      | [64]      |
| Optimised 'D'            | 0.047 | 0.4      | 1.5  | 11.1  | 8.6   | 0.3   |         | 94         |                      | [83]      |
| A6                       | 0.08  | 0.19     | 0.89 | 14.7  | 0.27  | 0.04  |         | 360        | 0.244                | [23, 90]  |
| B5                       | 0.04  | 0.19     | 0.86 | 13    | 1.7   | 0.04  |         | 300        | 0.578                |           |
| C5                       | 0.05  | 0.22     | 0.41 | 3     | 13.2  | 0.35  |         | 270        | 0.57                 |           |
| Camalloy 4/2b            | 0.014 | 0.76     | 1.36 | 12.66 | 5.24  | 0.1   | 0.053Ti | 216        | 0.47                 | [36, 99]  |
| LTTW                     | 0.04  | 0.32     | 0.36 |       | 11.9  |       |         |            |                      | [91]      |
| A                        | 0.042 | 0.22     | 0.65 | 10.91 | 9.37  | 0.26  |         | 194        |                      | [82]      |
| B                        | 0.035 | 0.25     | 0.43 | 12    | 5.26  | 0.46  |         | 320        |                      |           |
| A                        | 0.046 | 0.22     | 0.69 | 11.05 | 9.51  | 0.296 |         | 122        |                      | [95, 100] |
| B                        | 0.048 | 0.23     | 0.67 | 11.03 | 6.49  | 0.307 |         | 220        |                      |           |
| R                        | 0.046 | 0.22     | 0.7  | 12.54 | 9.48  | 0.298 |         | 60         |                      |           |
| O                        | 0.025 | 0.32     | 0.7  | 10    | 10    | 0.13  |         | 210        |                      |           |
| C13N                     | 0.029 | 0.15     | 0.19 | 15.66 | 7.07  | -     |         | 250        |                      | [92]      |
| C15N                     | 0.024 | 0.15     | 0.19 | 12.98 | 8.9   | -     |         | 250        |                      |           |
| XTT8                     | 0.04  | 0.26     | 0.56 | 7.6   | 10    | 0.47  |         | 209        |                      | [10]      |
| XTT10                    | 0.05  | 0.21     | 0.61 | 5.9   | 7.8   | 0.5   |         | 295        |                      |           |

|  |        |      |      |            |       |        |            |     |  |                 |
|--|--------|------|------|------------|-------|--------|------------|-----|--|-----------------|
| LTTE1  | 0.04   | 0.17 | 0.27 | 10.69      | 10.01 | 0.04   |            | 79  |  | [33]            |
| LTTE2  | 0.04   | 0.17 | 0.3  | 10.51      | 9.62  | 0.05   |            | 144 |  |                 |
| LTTE3  | 0.07   | 0.23 | 1.25 | 9.1        | 8.46  | 0.05   |            | 191 |  | [33, 101]       |
| '410NiMo'<br>LTT filler<br>alloy (bead<br>centre<br>measurement) | 0.020  | 0.34 | 0.48 | 12.5       | 3.8   | 0.47   | 0.06<br>Cu |     |  | [79]            |
| LTT 'weld 1'<br>Nom. 8% Ni<br>alloy                              | 0.07   | 0.45 | 1.05 | 9.52       | 7.33  | < 0.02 |            |     |  | [84, 93,<br>94] |
| LTT 'weld 1'<br>Nom. 10% Ni<br>alloy                             | 0.06   | 0.45 | 1.05 | 9.57       | 9.44  | < 0.02 |            |     |  |                 |
| LTT 'weld 1'<br>Nom. 12% Ni<br>alloy                             | 0.08   | 0.40 | 1.00 | 9.19       | 10.81 | < 0.02 |            |     |  |                 |
| LTT-C  | 0.014  | 0.7  | 1.27 | 13.4       | 6.1   | 0.07   |            | 281 |  | [70]            |
| LTT-S  | <0.020 | <1.0 | <2.0 | 15 -<br>18 | 6 - 8 | <2.0   |            | 221 |  |                 |
| <b>Standard<br/>weld</b>   |        |      |      |            |       |        |            |     |  |                 |
| OK 75/78   | 0.05   | 0.19 | 2.0  | 0.4        | 3.1   | 0.6    |            |     |  | [8, 102]        |
| OK Autorod<br>89   | 0.09   | 0.8  | 1.9  | 0.3        | 2.2   | 0.6    |            |     |  | [70]            |
| <b>Base Metal</b>  |        |      |      |            |       |        |            |     |  |                 |
| Weldox 960   | 0.20   | 0.50 | 1.6  | 0.7        | 2.0   | 0.7    | 0.3Cu      |     |  | [8, 102]        |

Table 2

**Table 2:** Mechanical properties of LTT weld metals from various sources [21, 23, 64, 66, 92, 96].

| Weld Metal            | 0.2% PS (MPa) | UTS (MPa)  | Elong. (%) | Impact toughness (J) |       |       |    |      | Ref.         |
|-----------------------|---------------|------------|------------|----------------------|-------|-------|----|------|--------------|
|                       |               |            |            | -40°C                | -30°C | -20°C | 0  | 20°C |              |
| 10Cr-10Ni             | 822           | 1192       | 36         |                      |       | 48    |    |      | [66]         |
| 10Cr-10Ni             | 708           | 1021       | 7          |                      |       |       |    |      | [96]         |
| B206/ OK Tubrod 15.55 | 700-850       | 950-1050   | >15        | >100                 |       |       |    | >110 |              |
| 13Cr/LC35             | 680           | 1050       | 15         | 30                   |       |       |    | 36   | [64]         |
| A6                    | 500           | 624        |            |                      |       |       | 8  | 10   | [96]<br>[23] |
| B5                    | 886           | 1002       |            |                      |       |       | 12 | 14   |              |
| C5                    | 702           | 1155       |            |                      |       |       | 14 | 14   |              |
| Camalloy 4/2b         | 838           | 1069       | 17.6       |                      |       | 53    |    | 72   | [36]         |
| LTTE(3)               | 1135          | 1287       | 6          |                      | 17    | 15    |    | 20   | [21]         |
| Series B              |               |            |            |                      | 22    | 27    |    | 28   |              |
| C13N                  | 495           | 1051       | 7          |                      |       |       |    |      | [92]         |
| C15N                  | 671           | 1117       | 7.7        |                      |       |       |    |      |              |
| <b>Standard Weld</b>  |               |            |            |                      |       |       |    |      |              |
| OK 75/78              | ~ 1100        |            |            | 79                   |       | 90    |    | 96   | [21]         |
| <b>Base Metal</b>     |               |            |            |                      |       |       |    |      |              |
| Weldox 960            | > 960         | 980 - 1150 | > 12       |                      | 27    | 27-30 |    |      | [21]         |

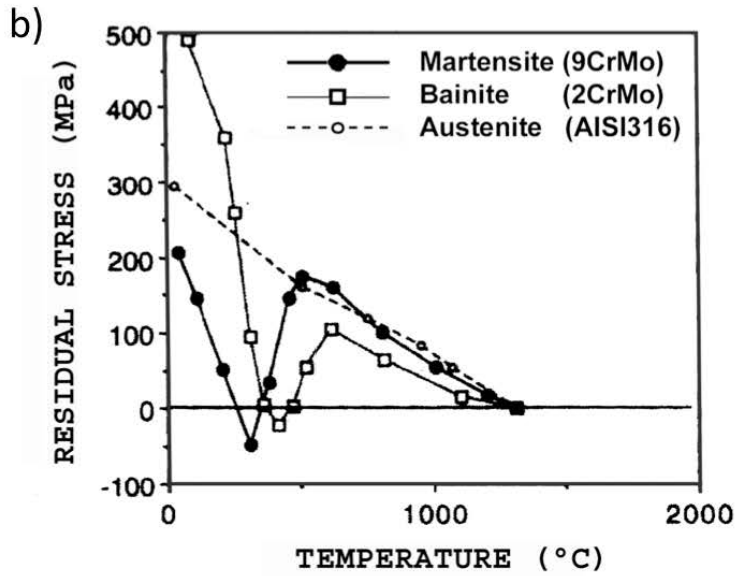
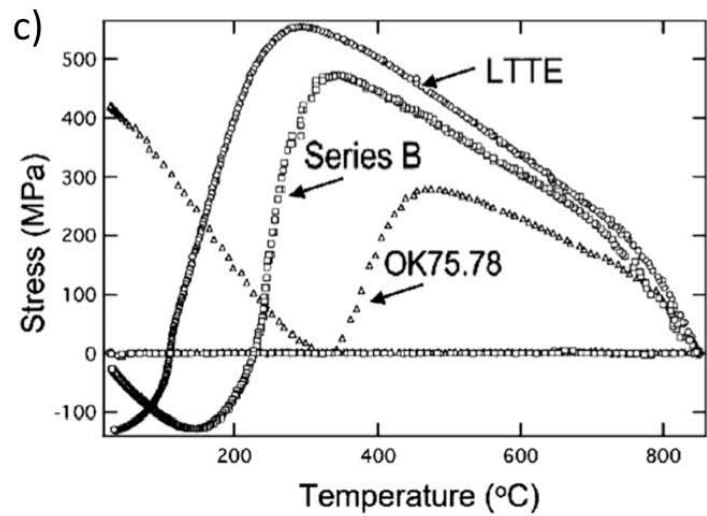
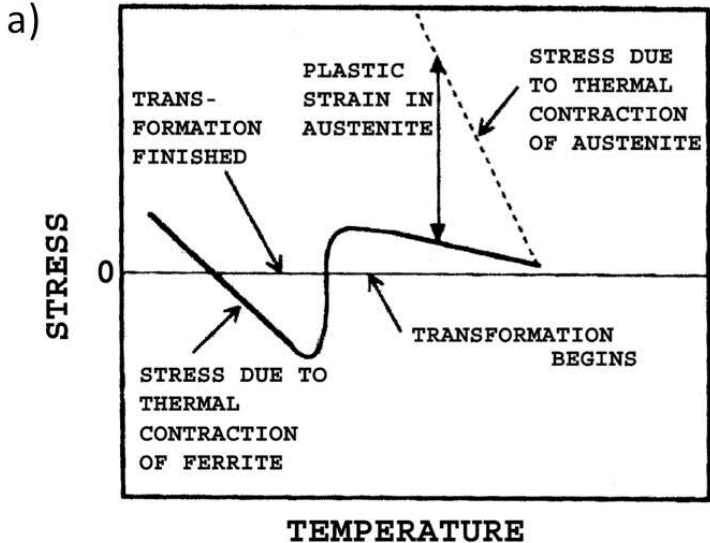
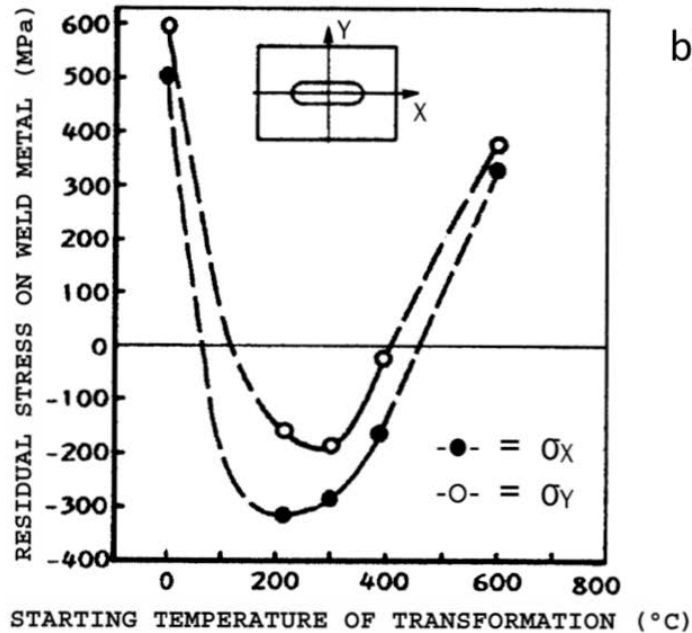
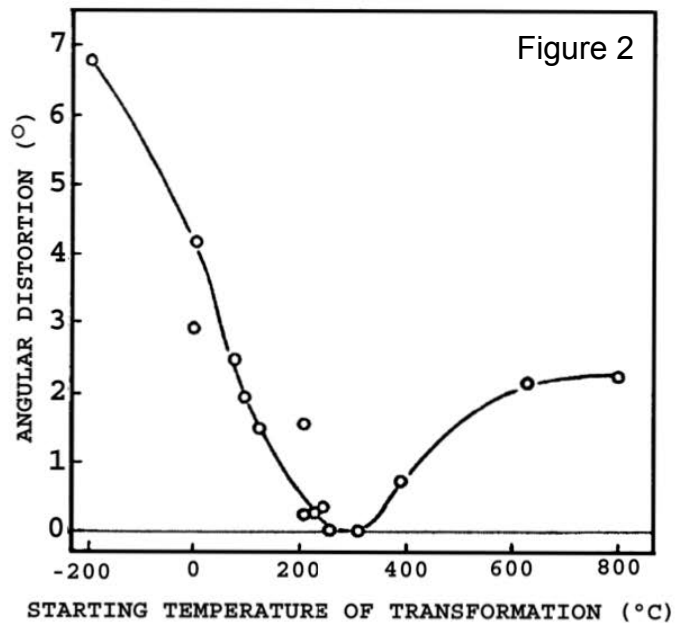


Figure 1

a)



b)



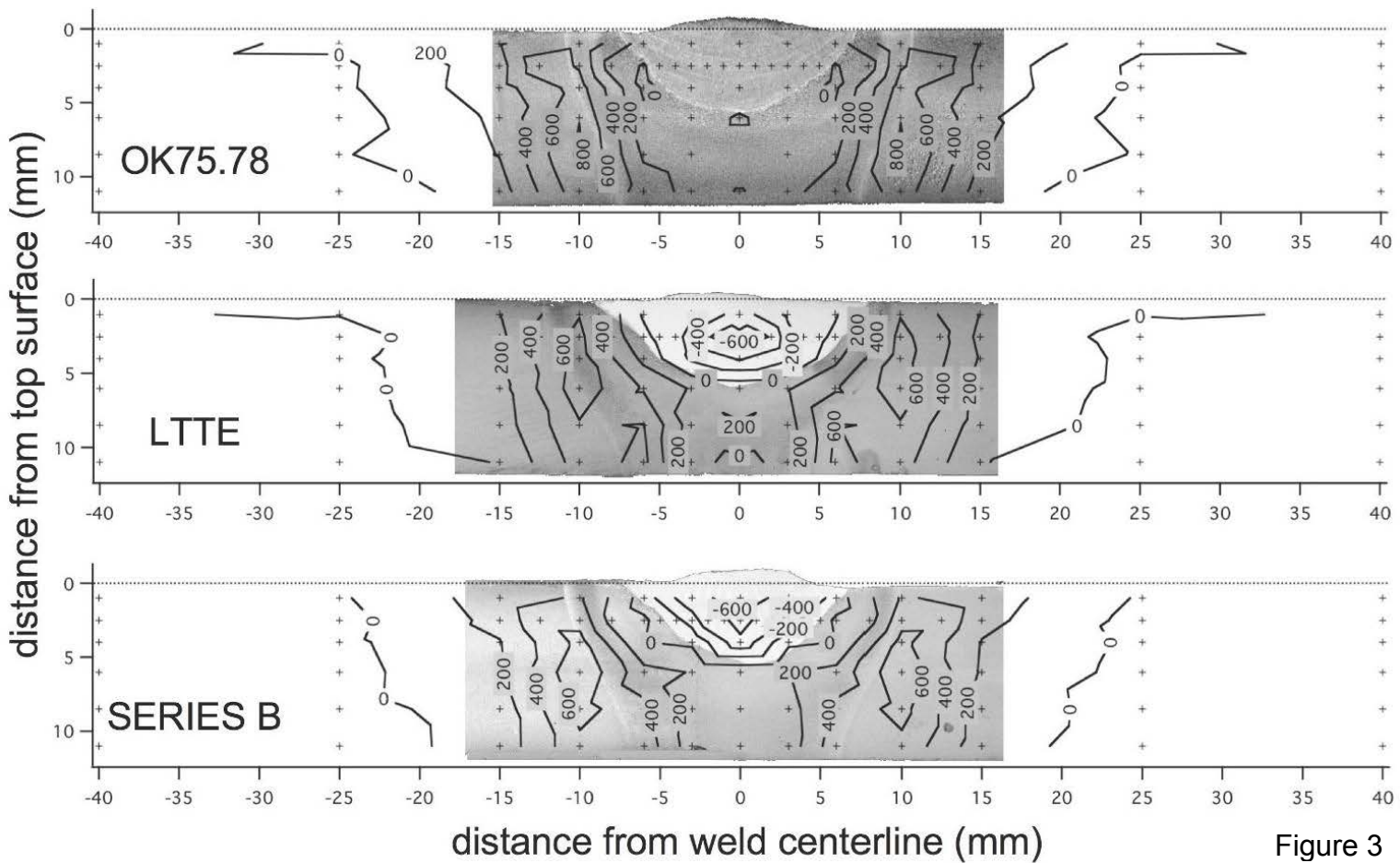


Figure 3

Stress Range (MPa)

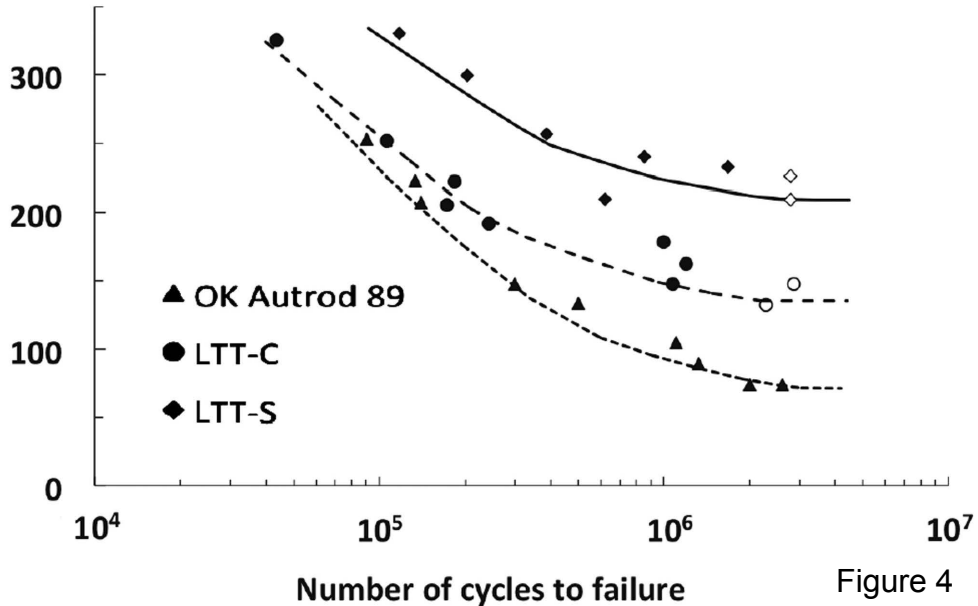


Figure 4

Fatigue strength at  $2 \times 10^6$  cycles,

$\Delta \sigma$  (MPa)

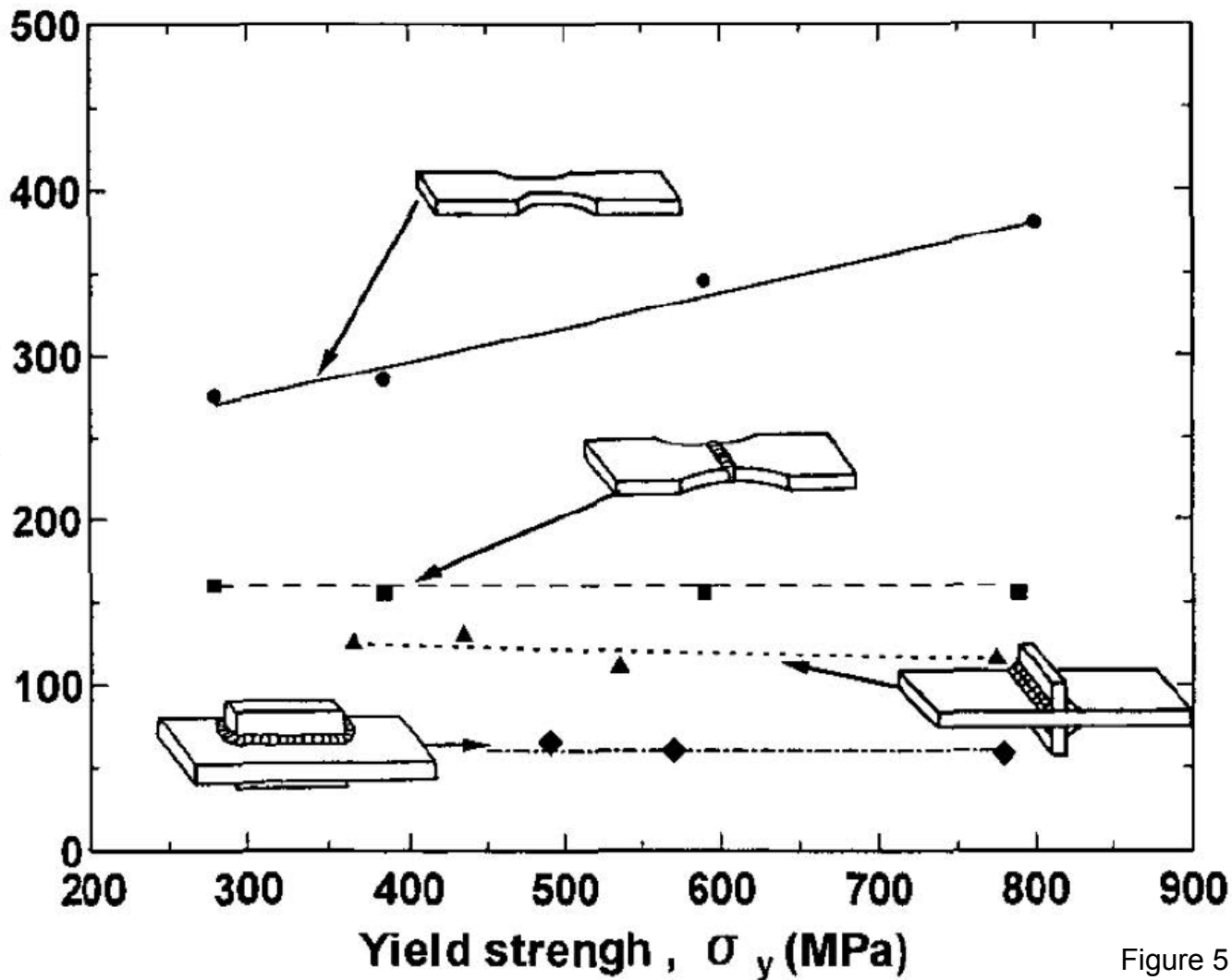


Figure 5

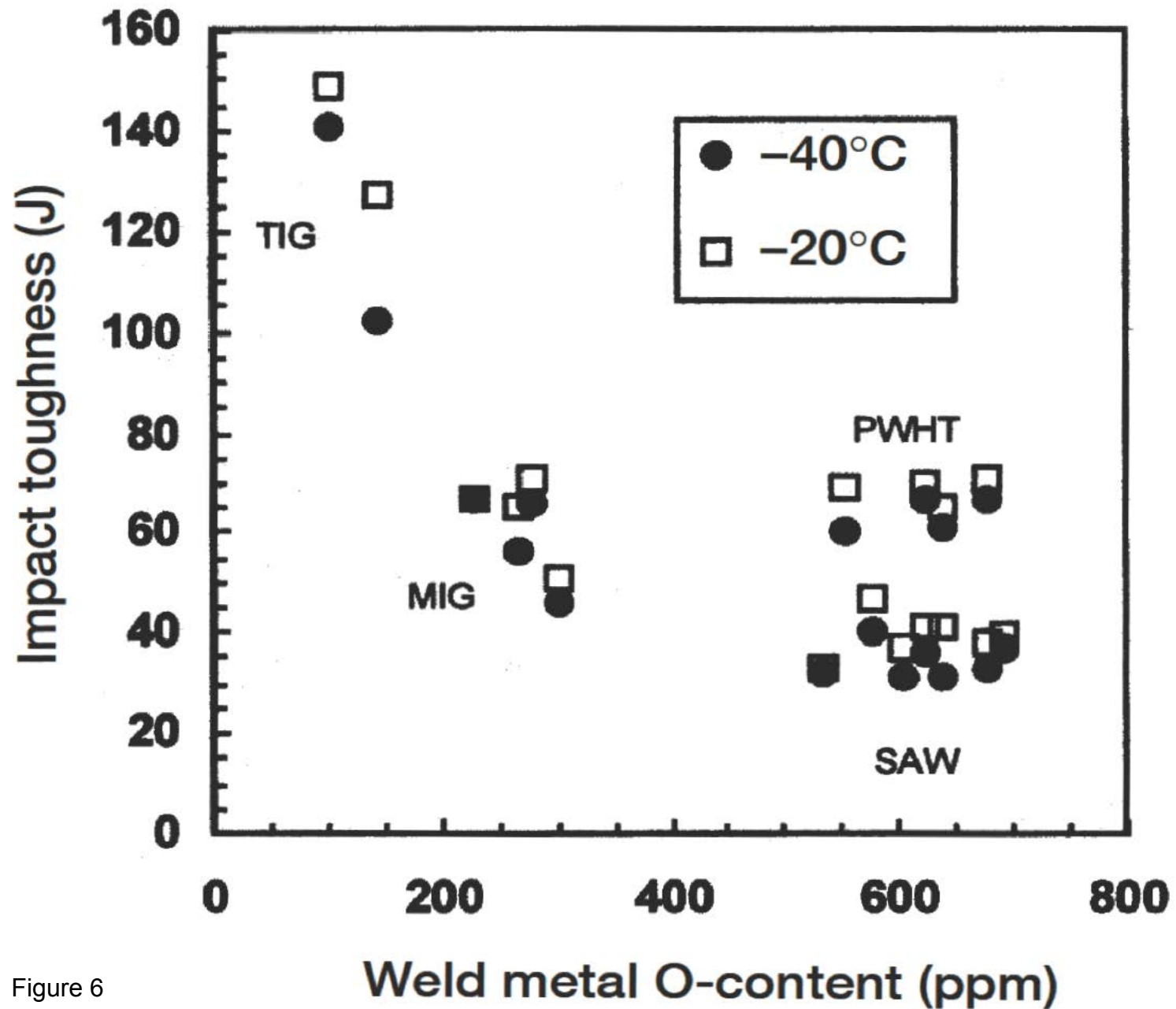


Figure 6